

is generally oxidized to H_2SO_4 with each molecule having the potential to contribute two hydrogen ions. Similarly each molecule of NO_2 deposited can yield one hydrogen ion.

The relative proportions of these components contributing to acid deposition to a hypothetical cereal crop in southern England are shown in Table 3. Dry deposited SO_2 comprises the greatest fraction of the deposited acidity followed by the contribution from HNO_3 , and the magnitudes of all the dry deposited species are individually larger than the 'acid rain' component.

These simple estimates serve to underline the importance of dry deposition mechanisms in the direct transfer of strong acids to vegetation surface structures. The aerodynamic resistance to transfer to forests and cities is considerably smaller than that for cereal crops. If similar (or even higher) concentrations of HNO_3 were maintained the deposition of these species would be correspondingly increased.

This work was supported by the Department of the Environment. We are grateful to J. A. Garland for advice and discussions.

Received 11 June 1986; accepted 9 February 1987.

1. Cox, R. A. *J. Photochem.* **25**, 43–48 (1984).
2. Cox, R. A. & Penkett, S. A. in *Acid Deposition* (eds Beilke, S. & Elshout, A. J.) 58–83 (CEC, Brussels, 1983).
3. UK Acid Rain Review Group Report (Warren Spring Laboratory, Stevenage, 1983).
4. Goldan, P. D. et al. *Atmos. Environ.* **17**, 1355–1364 (1983).
5. Grosjean, D. *Anal. Lett.* **15**, (A9) 785–796 (1982).
6. Eggleton, A. E. J. & Atkins, D. H. F. *Results of the Teeside Investigation UKAEA Report AERE-R 6983* (HMSO, London, 1972).
7. Appel, B. R., Tokiwa, T. & Haik, M. *Atmos. Environ.* **15**, 283–289 (1981).
8. Harrison, R. M. & Pio, C. A. *Tellus* **35B**, 155–159 (1983).
9. Stelson, A. W., Frieslander, S. K. & Seinfeld, J. H. *Atmos. Environ.* **13**, 369–371 (1979).
10. Huebert, B. J. & Robert, C. H. *J. geophys. Res.* **90**, (D1) 2085–2090 (1985).
11. Garland, J. A. & Derwent, R. G. *Q. J. R. met. Soc.* **105**, 169–183 (1979).
12. Garland, J. A. & Penkett, S. A. *Atmos. Environ.* **10**, 1127–1131 (1976).
13. Cox, R. A., Derwent, R. G. & Sandalls, F. J. *Some air pollution measurements made at Harwell, Oxfordshire during 1973–1975*. UKAEA Report AERE-R 8329 (HMSO, London, 1976).
14. Huebert, B. J. in *Precipitation Scavenging, dry deposition and resuspension Vol. 2* (Coordinators Pruppacher, H.R. Semonin, R. G. & Slinn, W. G. N.) 785–793 (Elsevier, New York, 1983).
15. Grennfelt, P. *Atmos. Environ.* **14**, 311–316 (1980).
16. Meixner, F. X., Muller, K. P., Aheimer, G. & Hofken, K. D. Proc. COST action 611 Meet: 'Pollutant cycles and transport: modelling and field experiments' (eds de Leuw, F. A. M. & van Emden, N. D.) 103–119 (RIVM Bilthoven, Netherlands, 1985).
17. Garland, J. A. Proc. R. Soc. **A354**, 245–268 (1977).
18. Schmelz, G. A. *Atmos. Environ.* **14**, 983–1011 (1980).
19. Meixner, F. X. in Proc. 2nd Meet. on Atmosphere Biosphere Interactions Mainz, 1986 (in the press).

The dependence of hurricane intensity on climate

Kerry A. Emanuel

Center for Meteorology and Physical Oceanography,
Massachusetts Institute of Technology, Cambridge,
Massachusetts 02139, USA

Tropical cyclones rank with earthquakes as the major geophysical causes of loss of life and property¹. It is therefore of practical as well as scientific interest to estimate the changes in tropical cyclone frequency and intensity that might result from short-term man-induced alterations of the climate². In this spirit we use a simple Carnot cycle model to estimate the maximum intensity of tropical cyclones under the somewhat warmer conditions expected to result from increased atmospheric CO_2 content. Estimates based on August mean conditions over the tropical oceans predicted by a general circulation model with twice the present CO_2 content yield a 40–50% increase in the destructive potential of hurricanes.

We shall first review a simple model³ of the mature tropical cyclone that is capable of predicting the maximum intensity that can be achieved by such storms as a function of environmental conditions. We then apply this model to the estimation of maximum cyclone intensity under a range of climates, and to a

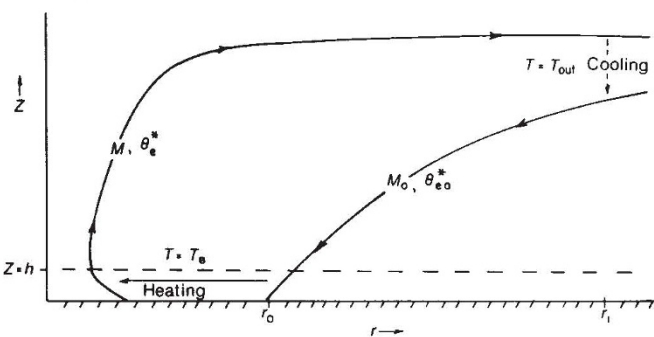


Fig. 1 Carnot cycle of the mature tropical cyclone³. Air begins with absolute angular momentum per unit mass M_0 and moist entropy θ_{ea}^* at a radius r_0 , and flows inward at constant temperature T_B within a thin boundary layer, where it loses angular momentum and gains moist entropy from the sea surface. It then ascends and flows outward to large radii, preserving its angular momentum (M) and moist entropy (θ_e^*). Eventually, at large radii, the air loses moist entropy by radiative cooling to space at a mean temperature T_{out} and acquires angular momentum by interaction with the environment.

specific situation predicted by a general circulation model simulation with increased atmospheric CO_2 .

Tropical cyclones make textbook examples of the operation of a Carnot engine, with the provision that the heat input is largely in the form of the latent heat of vaporization. Figure 1 illustrates the energy cycle³. At some radius r_0 (typically 100–500 km) surface air begins to flow inwards towards the cyclone centre within a frictional boundary layer whose depth is ~1 or 2 km. During its inward trek the air maintains a nearly constant temperature that is very close to the sea surface temperature but acquires water vapour from the ocean, which supplies the latent heat of vaporization. The rate at which it acquires latent heat is a monotonic function of the near-surface wind speed. As the air flows toward lower pressure, heat is added due to isothermal expansion as well. It is also during this inflow that air suffers the greatest frictional dissipation. At a much smaller radius (typically from 5 to 100 km) the air abruptly turns upward and ascends through the deep cumulo-nimbus clouds that constitute the eyewall. During this ascent the total heat content (sensible plus latent) is approximately conserved, though in the process there are large conversions of latent to sensible heat. There is also comparatively little frictional loss of energy in this branch. Finally, the air flows outward at the top of the storm and eventually loses the heat gained from the ocean by longwave radiation to space, and through friction re-acquires the lost angular momentum. This usually happens at some radius r_1 which is much larger than r_0 . Calculations are rather insensitive to the exact value of r_1 . The whole process is considered to take place in an atmosphere which is neutral to buoyant and centrifugal convection along angular momentum surfaces.

In the steady state, the mechanical energy available from this thermodynamic cycle balances frictional dissipation. As previously mentioned, the bulk of the latter occurs in the boundary layer inflow where air crosses surfaces of constant absolute angular momentum. (A much smaller amount occurs at large radii in the outflow.) The balance may be expressed symbolically

$$W_{BL} = \varepsilon \Delta Q \quad (1)$$

where W_{BL} is the work done against friction in the boundary layer, ΔQ is the total heat gain from the sea surface and ε is the thermodynamic efficiency, which is proportional to the difference between the temperature at which the heat is added (the sea surface temperature) and a weighted mean temperature at which it is lost in the upper atmosphere (see ref. 3 for an exact definition). The efficiency ε is largest in the tropics, where the depth of the moist convecting layer is large, and smaller at higher latitudes, approaching zero in many places.

Knowledge of the frictional loss in the boundary layer can be used to calculate the total drop in pressure in towards the eye of the storm through the use of Bernoulli's energy equation, which may be written

$$\frac{1}{2}\Delta v^2 + \int \alpha dp + W_{BL} = 0 \quad (2)$$

where $\frac{1}{2}\Delta v^2$ is the total change in kinetic energy per unit mass following the air flowing inward in the boundary layer, α is the volume per unit mass and p is the pressure. Since v is approximately zero at the beginning of the inflow (at r_0) and is exactly zero at $r=0$, Bernoulli's equation integrated all the way into the centre of the storm may be expressed

$$\int_{r_0}^0 \alpha dp = -\varepsilon \Delta Q, \quad (3)$$

where we have used equation (1) for W_{BL} . Using the ideal gas law to express α as a function of p and T (and water vapour content, which is variable), the author³ showed that the integral in equation (3) can be evaluated exactly. Specifically, both α and ΔQ can be regarded as functions of temperature, pressure and relative humidity (RH), so that equation (3) has the functional form

$$\Delta G(p, T, RH) = \varepsilon \Delta F(p, T, RH) \quad (4)$$

(The exact form is given by equation (21) of ref. 3.) To a very good approximation, the temperature is a constant equal to the sea surface temperature. Moreover, the relative humidity cannot exceed unity. This permits an evaluation, using equation (4), of the maximum possible pressure drop in towards the eye as a function of the sea surface temperature, the ambient relative humidity, and the thermodynamic efficiency ε , the last of which can be calculated from a knowledge of the ambient temperature structure of the atmosphere.

Figure 2 shows the results of a calculation of this kind using September mean sea surface temperatures, relative humidities, and temperature profiles used in calculating ε . Also shown are the measured central surface pressures of several of the most intense tropical cyclones recorded. As storms in these regions tend to move towards the north-west, they often reach maximum intensity on the downstream side of the region of maximum potential intensity. Apparently, the dynamics of tropical storms sometimes permit them to achieve the maximum intensity that is energetically possible. The central pressure (or more precisely the difference between the ambient and central pressures) is a good measure of storm intensity and is also closely related to the maximum wind speeds in tropical cyclones⁴.

The pattern of maximum intensity in Fig. 2 strongly resembles the September mean sea surface temperature distribution, although the relationship is highly nonlinear. This is because the thermodynamic efficiency, ε , is itself mostly a function of sea surface temperature since the depth of the moist convecting layer is large over relatively warm water and small over colder

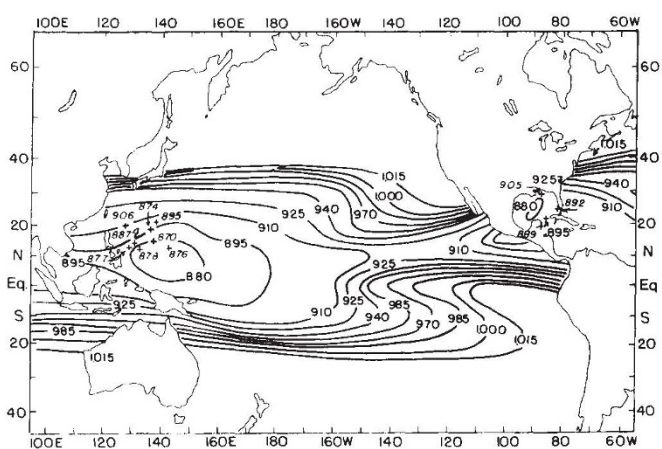


Fig. 2 Minimum sustainable central pressures (mb) under September mean climatological conditions, assuming an ambient pressure of 1,015 mb (ref. 3). Crosses mark the positions and central pressures of some of the most intense tropical cyclones on record¹.

water. The prediction of maximum cyclone intensity is therefore crucially dependent on estimates of sea water temperature. We next argue that changes in cyclone intensity due to climatic changes in ε and ambient relative humidity will be small.

Fractional changes in ε result from changes in the air temperature near the sea surface (T_B) and changes in the mean temperature of the ambient atmosphere at the levels where air flows out of the top of the storms (\bar{T}_{out}). The latter is typically the temperature of the lower stratosphere when ε is large. From the definition of ε

$$\frac{d\varepsilon}{\varepsilon} = \frac{1}{T_B - \bar{T}_{out}} \left[\frac{\bar{T}_{out}}{T_B} dT_B - d\bar{T}_{out} \right] \quad (5)$$

We are principally concerned about regions of the Earth where tropical cyclones are particularly frequent and intense; these are characterized by relatively large values of $T_B - \bar{T}_{out}$. Since this quantity has a typical magnitude of ~ 100 °C, the percentage change in ε will be nearly equal to the quantity in brackets in equation (5). As an upper bound on this change, consider a situation in which \bar{T}_{out} changes but T_B remains fixed. It follows that a change of 4 °C in \bar{T}_{out} would result in only about a 4% change in ε . In fact, dT_B and $d\bar{T}_{out}$ are positively correlated in virtually all climate simulations performed to date. In the particular simulation discussed later in this letter, dT_B and $d\bar{T}_{out}$ are about equal. This makes fractional changes in ε , according to equation (5), more of the order of 1%, except where ε is initially small. We conclude that changes in the thermodynamic efficiency resulting from modest climate change would be insignificant.

The Carnot cycle model prediction of maximum intensity is quite sensitive to the relative humidity of near-surface air. The predictions of this quantity in large-scale numerical models is very sensitive to physical assumptions about evaporation from the sea, cumulus convection, radiation, and so on. In fact, most models do not do very well at predicting relative humidity. Nature does not appear to be as sensitive, however, since the relative humidity over the ocean is remarkably constant over a wide range of sea surface temperatures, cloud cover and precipitation. It varies from nearly 75% over colder ocean waters in middle latitudes to about 80% in the main tropical cyclone-producing regions. In many of the simpler climate models a fixed relative humidity is assumed. In view of these observations and lack of confidence in model predictions, we assume that the relative humidity over the tropical ocean remains fixed at the current values. This assumption also ties the temperature at each level in the troposphere to sea surface temperature.

With these assumptions, changes in maximum tropical cyc-

Table 1 Minimum sustainable central pressure and maximum wind speed as a function of sea surface temperature with $\varepsilon = 0.33$ and an ambient relative humidity of 78%. (Ambient pressure = 1,015 mbar)

T (°C)	P_c (mbar)	V_{max} (m s ⁻¹)
27	911	72
28	902	75
29	891	79
30	879	83
31	865	88
32	849	93
33	829	99
34	805	106

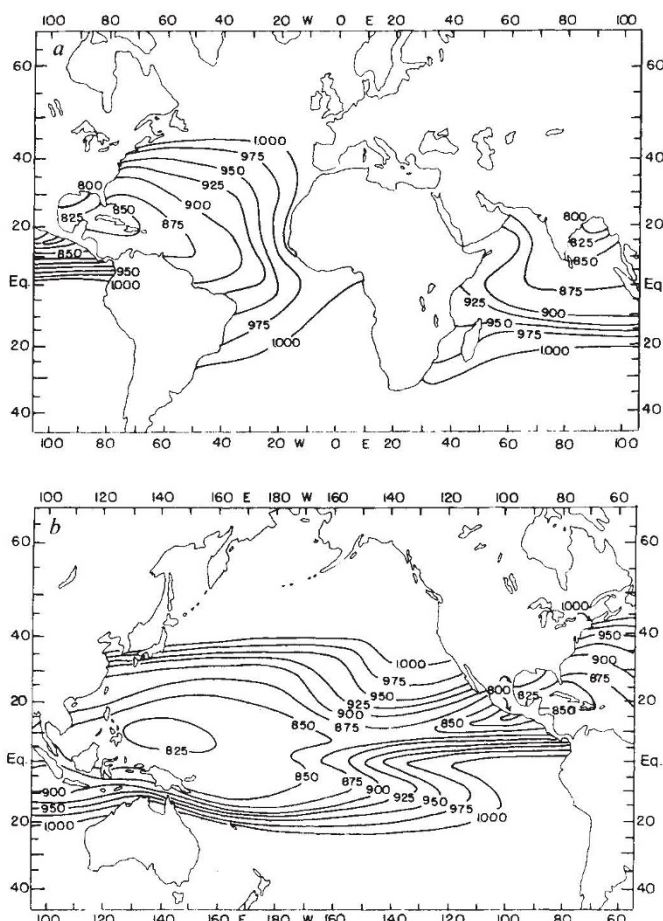


Fig. 3 Minimum sustainable central pressures (mb) as in Fig. 2, but using sea-surface temperature increases predicted by a general circulation model^{3,6} averaged over five Augusts in simulations with twice the present CO₂ content. *a*, Shows the Atlantic and Indian Oceans; *b*, the Pacific.

lone intensity are strictly related to changes in sea surface temperature. The Carnot cycle is particularly sensitive to sea surface temperature as the latent heat content of air at fixed relative humidity is a strongly exponential function of temperature, approximately doubling for each 10 °C increment of temperature above 0 °C. Table 1 shows the minimum sustainable central pressures of tropical cyclones as a function of sea surface temperature for a value of ϵ characteristic of the Caribbean and western Pacific tropical cyclone regions, assuming a surface relative humidity of 78% and an ambient surface pressure of 1,015 mb. Relatively small changes in sea surface temperature are associated with large intensity changes, with an increase of 3 °C leading to a 30–40% increase in the maximum pressure drop. Table 1 also shows estimates of the maximum wind speed in tropical cyclones based on empirical relations between wind and pressure developed by Holland⁴, taking his parameter 'B' to be 1.5. (The maximum wind is strictly bounded by the maximum pressure drop since the latter serves as the potential energy for inflowing air.) The wind increases as the square root of the pressure drop, yielding a 15–20% increase for an increase of 3 °C in sea surface temperature. The destructive potential of the wind, it should be added, varies as the square of the wind speed and thus as the total pressure drop.

To obtain some idea of the global distribution of the changes in maximum cyclone intensity that might result from predicted increases in atmospheric CO₂ we rely on predicted changes in sea surface temperature produced by the Goddard Institute for Space Studies General Circulation Model II described by

Hansen *et al.*⁵ with modifications to account for ocean mixed layer heat capacity and variable ice cover as described in ref. 6. Broadly, the model solves the conservation equations for energy, momentum, mass, and water and the equation of state on a coarse grid with a horizontal resolution of 8° latitude and 10° longitude, and with 9 layers in the vertical. The radiative scheme accounts for the radiatively significant atmospheric gases, aerosols and cloud particles, and cloud cover and height are predicted. Ground hydrology and surface albedo depend on local vegetation and snow and ice cover, which are predicted. The diurnal and seasonal cycles are included in the model. Ocean temperatures and ice cover are computed based on energy exchange between the atmosphere and an ocean mixed layer with specified heat capacity and advective heat transport. The last two vary with season at each grid point.

Figure 3 shows the minimum sustainable central pressures of tropical cyclones based on sea surface temperature changes predicted by the general circulation model averaged over five Augusts of a simulation with twice the present atmospheric CO₂ content. These changes, which in the tropics range between 2.3 °C and 4.8 °C, have been added to the current August climatological sea surface temperatures, while ϵ and surface relative humidity remain unchanged from the present climate. Minimum pressures are substantially lower in the tropics, especially in partially enclosed basins such as the Gulf of Mexico and the Bay of Bengal where minimum sustainable pressures are below 800 mbar. Were these sea surface temperature increases realized, the maximum destructive potential of tropical cyclones would be substantially increased, in some places by as much as 60%.

This analysis pertains only to the maximum sustainable pressure drop in tropical cyclones and has no direct implications for either the average intensity of cyclones or their frequency of occurrence. While one intuitively expects that average intensity increases with maximum intensity, the question of frequency is in fact poorly understood. Tropical cyclones do not arise spontaneously even under favourable conditions but appear to originate in disturbances whose origins derive from separate dynamical mechanisms, and will only do so under certain environmental conditions⁷. There is no obvious reason, however, to suppose that frequencies would be substantially diminished in a climate with doubled CO₂.

Several caveats should be mentioned regarding this analysis. In the present climate, only a small fraction of the total number of cyclones which form reach the maximum intensity given by this analysis, probably because of the relatively long spin-up time for storms of this kind, and the tendency for strong cyclonic circulations to induce upwelling of cold water. To these caveats we must add the relatively large uncertainties associated with climate simulations. In particular, the coupling of ocean dynamics to atmospheric circulation is presently quite crude. While better estimates of tropical cyclone intensities must await more sophisticated modelling efforts, the present analysis suggests that predicted climate changes associated with increased atmospheric CO₂ will lead to substantially enhanced tropical cyclone intensity.

I thank James Hansen, Gary Russell and Reto Ruedy of the NASA Goddard Space Flight Center Institute for Space Studies, and Peter Stone of MIT. The work was completed with the assistance of NSF Grant ATM-8513871.

Received 27 October; accepted 31 December 1986.

- Anthes, A. R. *Tropical Cyclones: Their Evolution, Structure and Effects* (American Meteorological Society, Boston, 1982).
- National Research Council (eds) *Changing Climate*, (National Academy Press, Washington, 1983).
- Emanuel, K. A. *J. atmos. Sci.* **43**, 585–604 (1986).
- Holland, G. J. *Mon. Weath. Rev.* **108**, 1212–1218 (1980).
- Hansen, J. *et al.* *Mon. Weath. Rev.* **111**, 609–662 (1983).
- Hansen, J. *et al.* in *Climate Processes and Climate Sensitivity* (eds Hansen, J. E. & Takahashi, T.) 368 (American Geophysical Union, Washington, 1984).
- Gray, W. M. in *Intense Atmospheric Vortices* (eds Bengtsson, L. & Lighthill, J.) 3–20 (Springer, New York, 1982).